Electronic Supplementary Information

Wavelength-switchable photocurrent in a hybrid TiO_2/Ag nanocluster photoelectrode

Hongjun Chen,[†] Qiong Wang,[†] Miaoqiang Lyu,[†] Zhi Zhang,[§] Lianzhou Wang [†*]

[†]Nanomaterials Centre, School of Chemical Engineering and Australian Institute for Bioengineering and Nanotechnology, The University of Queensland, QLD 4072, Australia.
[§]Materials Engineering, The University of Queensland, QLD 4072, Australia.
Fax: (+) 61 7 33654199; E-mail: l.wang@uq.edu.au

Experimental Section:

Chemicals. $NaSO_4$, $AgNO_3$, (3-mercaptopropyl)trimethoxysilane and poly(methacrylic acid) was purchased from Sigma-Aldrich and was used as received without further purification. The water used was purified through a Millipore system.

The fabrication procedure. As shown in scheme 1, a typical mesoporous FTO/TiO_2/Ag NCs photoelectrode was fabricated as follow. One layer of TiO_2 paste (Dyesol Company) was deposited on conductive surface of FTO by doctor-blade method and then sintered at 450 ℃ for 30 min. Then the obtained FTO/TiO_2 photoelectrode was immersed into Ag NCs solution for 24 h to obtain FTO/TiO_2/Ag NCs photoelectrode. The Ag NCs solution was prepared according to reference.[9] After thoroughly rushing the surface by Millipore water, the FTO/TiO_2/Ag NCs photoelectrode was directly used for photoelectrochemical measurements.

Instrumentation. The UV-vis absorption spectra were recorded with a V650 spectrophotometer (JASCO). The X-ray diffraction (XRD) patterns were collected on a diffractometer (Miniflex, Rigaku). X-ray photoelectron spectroscopy (XPS) was performed using an X-ray photoelectron spectrometer (a monochromatic Al KR X-ray source, Thermo Escalab 250). The transmission electron microscopy (TEM) was performed on Philips Tecnai F20, operated at 200 kV, equipped with X-ray energy dispersive spectroscopy (EDS) for compositional analysis. Scanning electron microscopy (SEM) and EDS measurement were performed on JEOL JSM-7001F.

Photoelectrochemical measurements. Photoelectrochemical measurements were performed in a home-made one-compartment reactor with a quartz window. A three-electrode configuration was used with Pt wire, Ag/AgCl electrode, and FTO/TiO_2/Ag NCs as the counter, reference, and working electrodes, respectively. N_2-saturated 1 M of $NaSO_4$ solution (pH = 6) was used as the electrolyte. Amperometric J-T curves were measured at 0 V vs. Ag/AgCl on an Electrochemical Workstation (CHI660d). A xenon lamp (150 W, Newport) with an AM 1.5G filter was used as the light source for the measuring the photocurrent. The illumination area was set by an aperture to 0.785 cm^2. The Mott–Schottky analysis was performed in a three-electrode configuration in 1 M $NaSO_4$ solution with 5 kHz frequency in the dark.

Supporting Figures

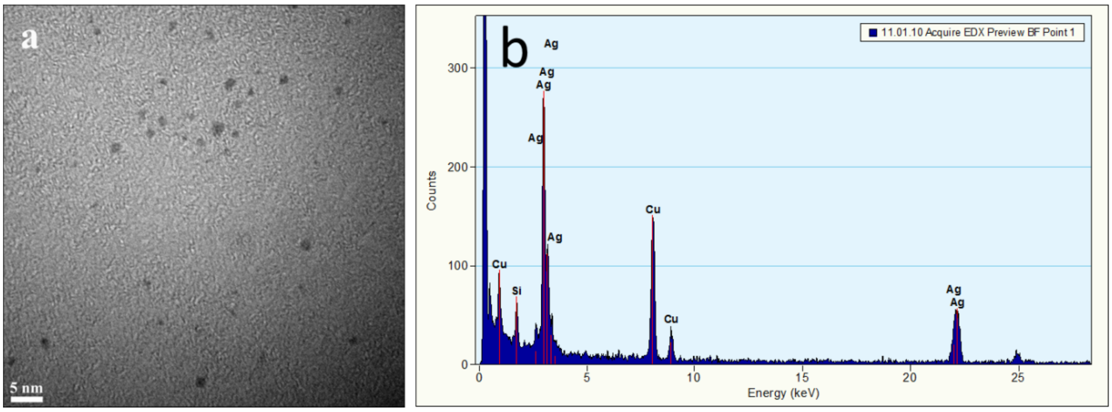

Fig. S1. Typical TEM image (a) and EDS (b) of Ag NCs.

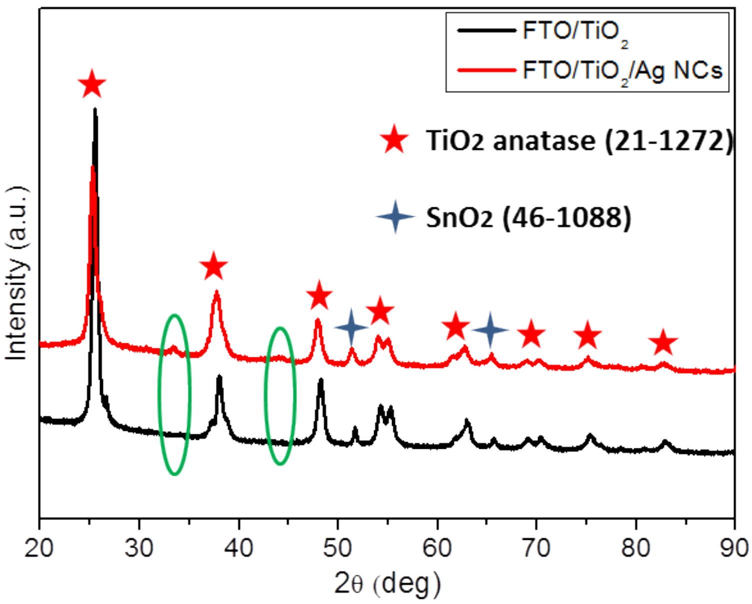

Fig. S2. XRD patterns of FTO/TiO$_2$ and FTO/TiO$_2$/Ag NCs photoelectrodes, the green circles indicate the weak difraction peaks of Ag NCs.

The XRD peaks of Ag are very weak, due to the very low content of Ag in the hybrid film (the atomic ratio of Ag in the hybrid film was only 3.22 at% based on the ICP measurement) and the very small size of Ag NCs (around 3 nm).

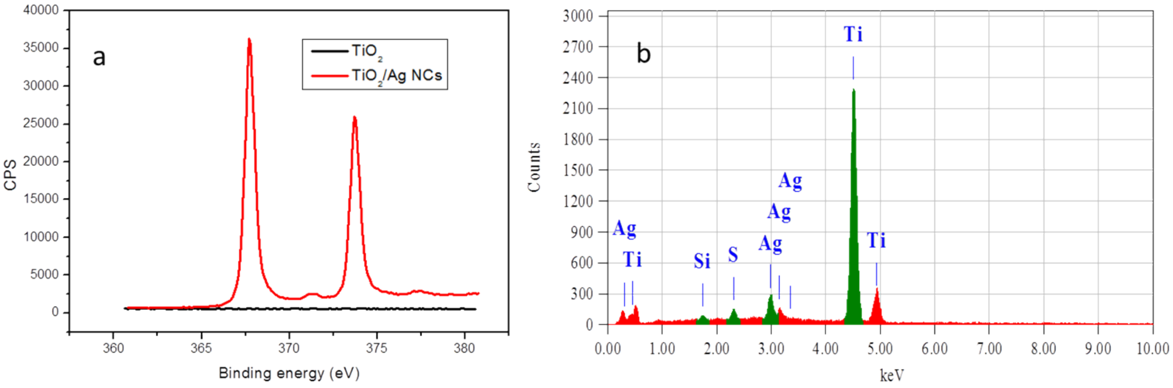

Fig. S3. High resolution XPS spectra of Ag (a) and EDS of FTO/TiO_2/Ag NCs photoelectrode (b).

The two weak peaks at the binding energy of *ca.* 371 and 377 eV can be attributed to the energy loss peaks, which is not associated with the Ag NCs.

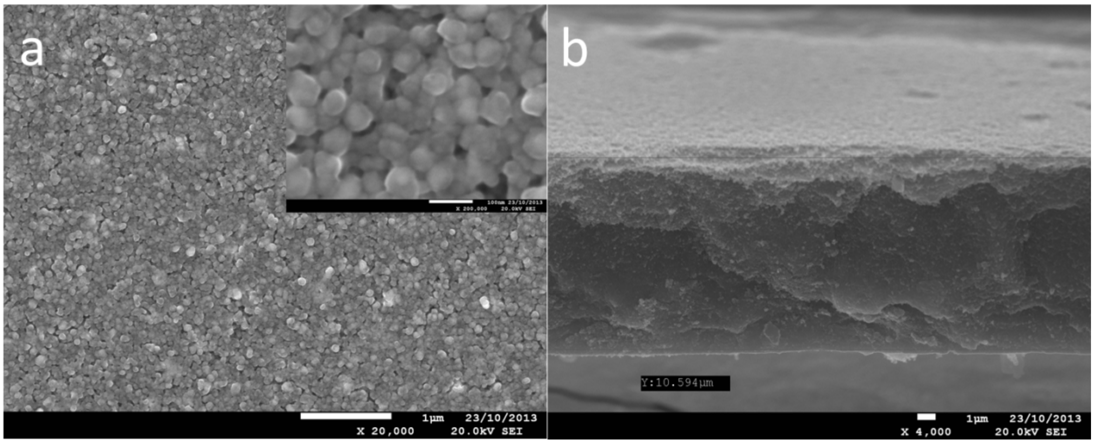

Fig. S4. Typical SEM images of FTO/TiO_2/Ag NCs with top-down (a) and cross-seciton (b) views, the inset in a is the enlarged SEM image.

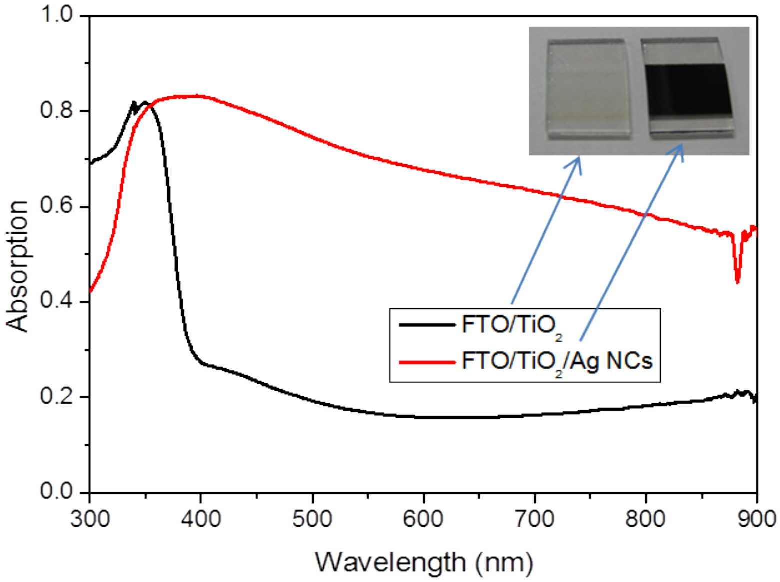

Fig. S5. UV-vis spectra of FTO/TiO_2 and FTO/ TiO_2/Ag NCs photoelectrodes , the inset is the image of FTO/TiO_2 and FTO/ TiO_2/Ag NCs photoelectrodes.

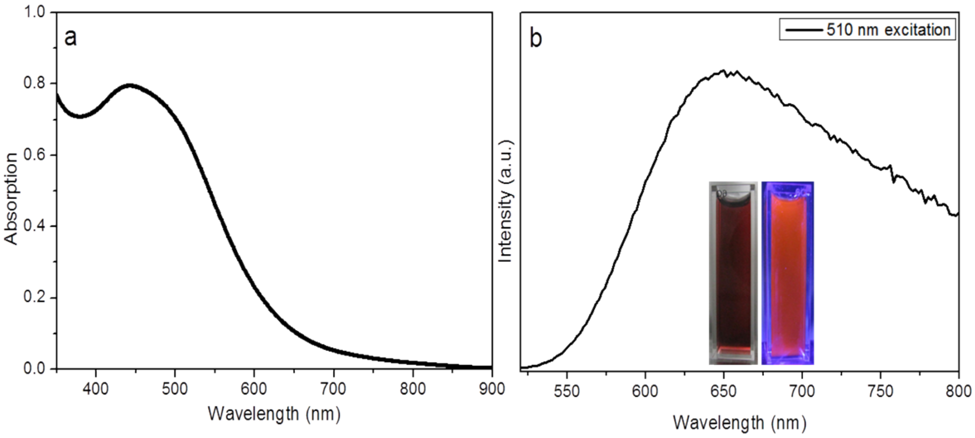

Fig. S6. UV-vis (a) and photoluminescence (b) spectra of the aqueous solution of the Ag NCs, the inset in Fig. S6b is the photographs of the Ag NCs solution under day light (left) and under UV lamp excitation (λ_{ex}= 365 nm) (right).

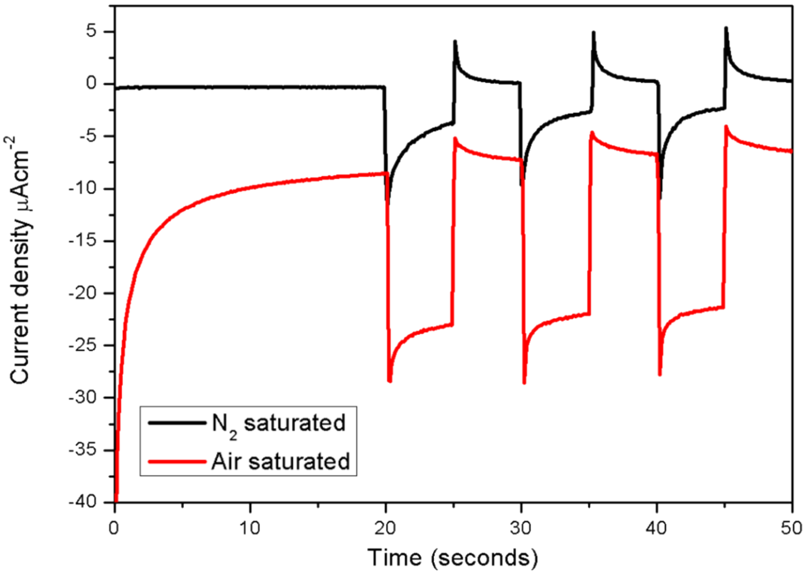

Fig. S7. J-T curves of FTO/TiO_2/Ag NCs measured in N_2- or air-saturated 1 M $NaSO_4$ solution under chopped light with filter glass > 455 nm. Applied potential was 0 V vs. Ag/AgCl.

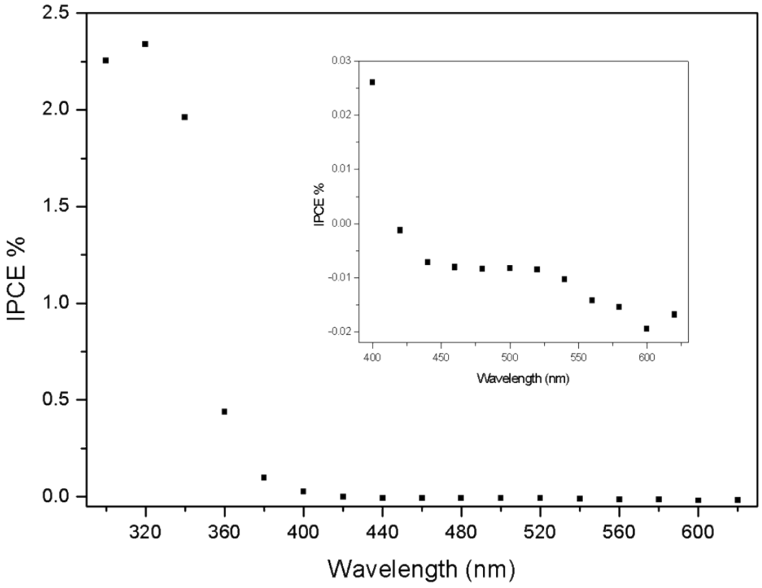

Fig. S8. IPCE value for the FTO/TiO_2/Ag NCs photoelectrode, the inset is the enlarged part from 400 to 620 nm.

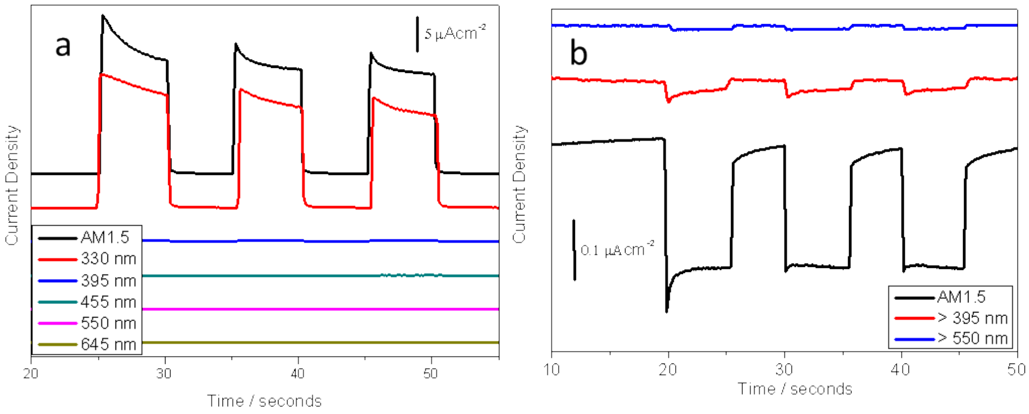

Fig. S9. I-T curves of FTO/TiO_2 (a) and bulk Au electrode/MPTMS/Ag NCs (b) under chopped light with different filter wavelengths. Applied potential was 0 V vs. Ag/AgCl.

The Ag NCs /Au electrode shows much smaller photocurrent density than that of TiO_2/Ag NCs photoelectrode. This is because the self-assembly fabrication was used for the preparation of Ag NCs/Au electrode and only single layer of Ag NCs can be absorbed on the surface of dense Au electrode. While much more Ag NCs can be loaded onto the surface of TiO_2 due to the mesoporous structure of the photoelectrode. From Fig. S4b, it can also be clearly seen that the thickness of the TiO_2 photoelectrode can reach around 10 um, which is much thicker than that of Ag NCs/MPTMS layer on Au electrode.

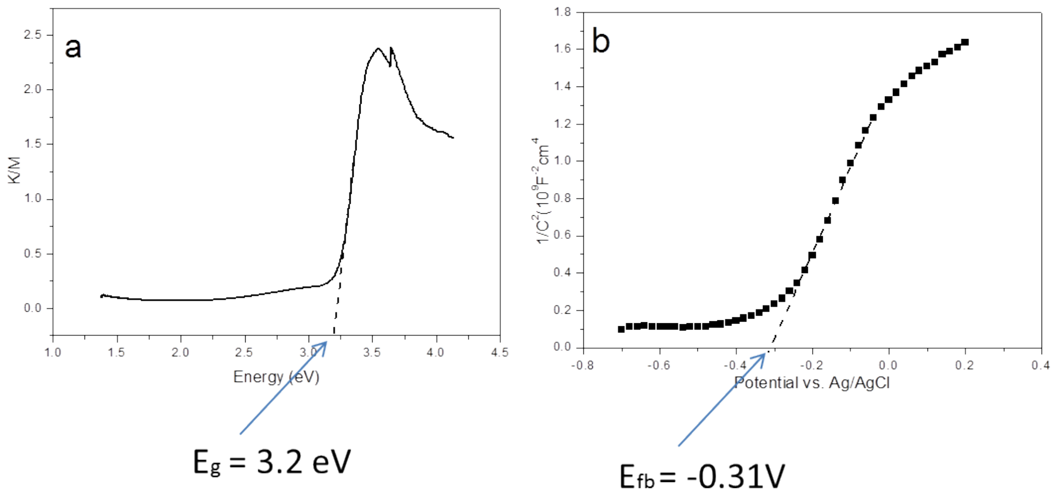

E_g = 3.2 eV

E_{fb} = -0.31V

Fig. S10. The K/M curve (a) and Mott-Schottky curve (b) of FTO/TiO_2.

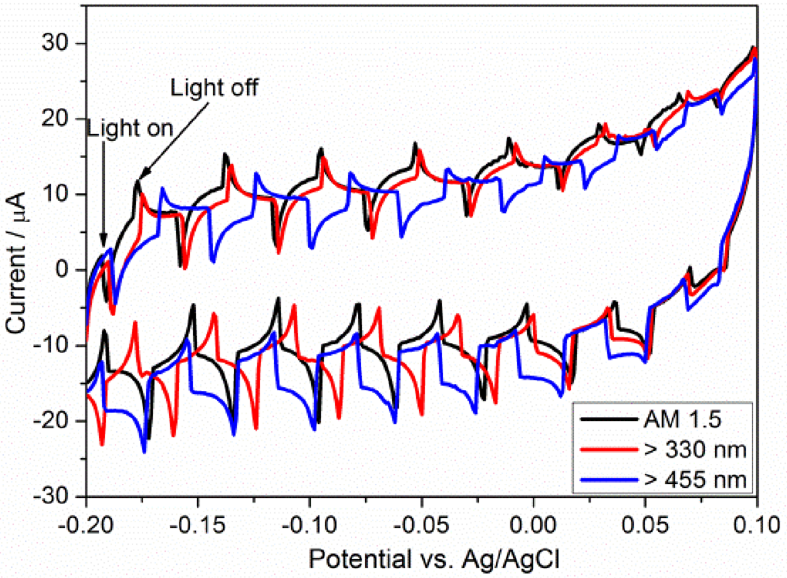

Fig. S11. CV curves of FTO/TiO_2/Ag NCs photoelectrode under chopped light (manually controlled) with different filter wavelengths (AM1.5, > 330 nm and > 455 nm).

As shown above, it is clear that the spike currents are much heavier when the applied potentials are more negative. Meanwhile, it is also found that the background current begins to greatly increase when the applied potential scans more positive (like from 0.05 to 0.1 V vs. Ag/AgCl), which may be ascribed to the beginning oxidation of Ag NCs. In order to inhibit the oxidation of Ag NCs, the scan potential range is no more positive than 0.1 V vs. Ag/AgCl.

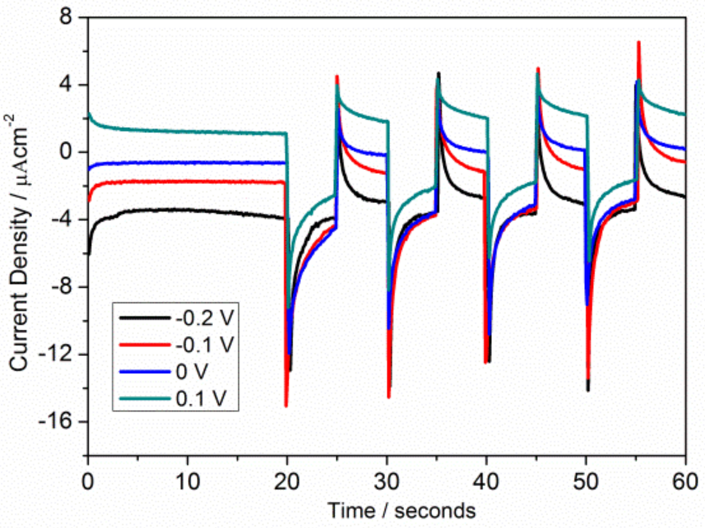

Fig. S12. J-T curves of FTO/TiO_2/Ag NCs photoelectrode under chopped light with filter wavelength >455 nm under different applied potentials.

The J-T curves of FTO/TiO_2/Ag NCs photoelectrode under chopped light with filter wavelength > 455 nm under different applied potentials are shown in Fig. S12. In this fig., the background current are gradually increased when the applied potentials are changed from negative to positive potential, which is in agreement with the discussion above (comment 1). Meanwhile, the transient photocurrent densities are also gradually increased when the applied potentials increased from -0.2 V to 0.1 V. In order to inhibit the slow oxidation of Ag NCs, the applied potential was chosen 0 V not 0.1 V although the transient photocurrent density at 0.1 V is slightly higher than that of 0 V.

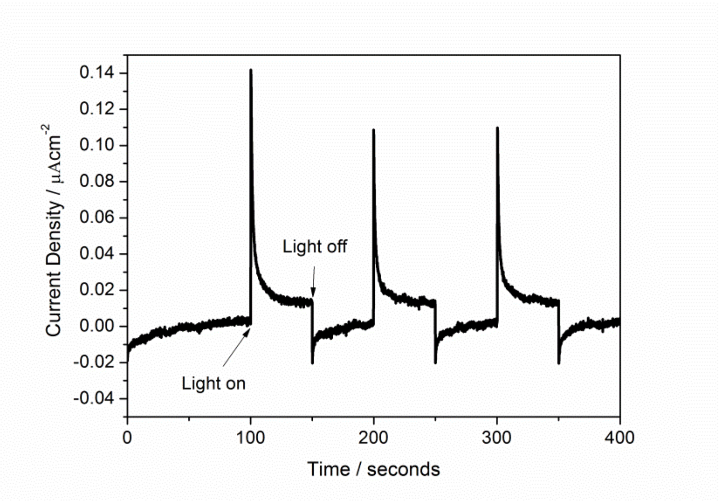

Fig. S13. J-T curves of Ag NCs modified on the dense TiO_2 layer under chopped light with filter wavelength >455 nm. Applied potential was 0 V vs. Ag/AgCl.

The TiO_2 dense layer was fabricated by sputtering the Ti with O_2 plasma on FTO substrate. Then the TiO_2/FTO substrate was calcinated at 450 °C for 1 hour under air to increase the crystallinity of TiO_2. Thus-obtained substrate was immersed into the Ag NCs solution for 24 h for the immobilization of the Ag NCs on the surface. As shown in Fig. S13, the Ag NCs/TiO_2/FTO substrate demonstrated anodic photocurrent under >495 nm illumination, which is totally different with the Fig. 1 in the manuscript. On the other side, it also verifies the statement that there is no potential gradient within mesoporous TiO_2 photoelectrode.

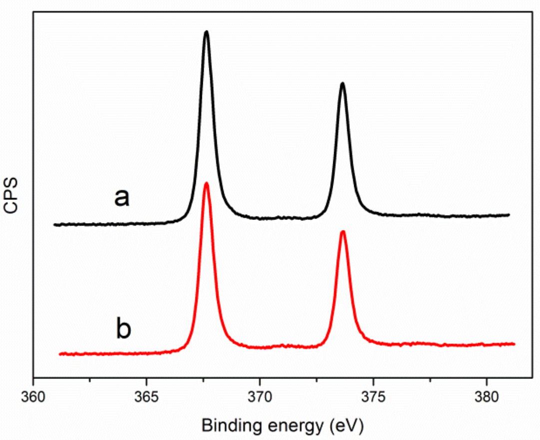

Fig. S14. High resolution XPS spectra of Ag before (a) and after 1 hour of illumination under AM 1.5. Applied potential was 0 V vs. Ag/AgCl.

We use the XPS to detect the valence state of Ag before and after 1 h illumination under AM 1.5 with the applied potential of 0 V. vs. Ag/AgCl. As shown in Fig. S14, the binding energy of Ag is not shifted and the energy difference between the Ag $3d_{5/2}$ and Ag $3d_{3/2}$ is still 6 eV after 1 h illumination. All of this suggests the Ag NCs are not be oxidized even under AM 1.5 illumination.